

Studies on the Valence State of Iron Atoms in the Mixed-Valence Binuclear Ferrocenes by X-Ray Absorption Near Edge Structure (XANES) and by X-Ray Photoelectron Spectroscopy (XPS)

Kumiko IWAI,* Makoto IWAI, Kyoko SUTO, Satoru NAKASHIMA,
Izumi MOTOYAMA, Hirotoishi SANO,* Isao IKEMOTO,
Nobuhiro KOSUGI,[†] and Haruo KURODA[†]

Department of Chemistry, Faculty of Science, Tokyo Metropolitan University,
Fukasawa, Setagaya-ku, Tokyo 158

[†]Department of Chemistry, Faculty of Science, The University of Tokyo,
Hongo, Bunkyo-ku, Tokyo 113

(Received September 12, 1985)

In order to study the valence state in the mixed-valence binuclear ferrocenes, X-ray absorption spectra near the Fe K-edge were measured using synchrotron radiation. Well-resolved lines in the spectra obtained for ferrocene derivatives were assigned to the $1s \rightarrow 3d$, $1s \rightarrow \text{Cp}(\pi^*)$, and $1s \rightarrow 4p$ transitions, respectively, based on the molecular orbitals. There is an apparent difference in the $1s \rightarrow 3d$ transitions between trapped-valence compounds and averaged-valence compounds in the I_3^- salts of the monocation of binuclear ferrocenes. The valence states of the mixed-valence binuclear ferrocenes were also studied by X-ray photoelectron spectroscopy.

Among polynuclear organometallic mixed-valence compounds, there exist metal ions having different formal oxidation states in their individual chemical species. A growing interest has been paid to such compounds in connection with studies of superconductive materials and of biological "mixed-valence" systems.¹⁾ The present authors have studied by Mössbauer spectroscopy the valence state for the salts of mono-oxidized binuclear ferrocene cations, in which two kinds of iron atoms, formally in the Fe(II) and Fe(III) states, are simultaneously present.^{2–4)}

Mössbauer spectra of the salts of mono-oxidized binuclear ferrocene cations are classified into two types; one is the trapped-valence type which contains ferrocene-like bivalent and ferrocenium-like trivalent atoms, as found in the case of triiodide salts of biferrocene⁵⁾ and 1',1'''-dichlorobiferrocene,⁴⁾ and the other is the averaged-valence type which contains two equivalent iron atoms, as in the case of triiodide salts of 1,1':1',1'''-biferrocenylene,⁶⁾ 1',1'''-dibromo- and 1',1'''-diiodobiferrocene.⁴⁾ It has been also reported that 1',1'''-diethyl- and 1',1'''-dipropylbiferrocenium⁺ I_3^- salts give rise to a transition from the averaged-valence state of iron atoms to the trapped-valence state as the temperature is lowered.⁷⁾ Although Mössbauer spectroscopy can distinguish whether or not the rate of the thermal electron transfer between two iron atoms is higher than ca. 10^{-7} s, no additional information from Mössbauer spectroscopy is available about the thermal electron transfer between the two atoms with a time scale faster than 10^{-7} s.

In the present study, X-ray absorption spectra near the edge structure (XANES) and X-ray photoelectron spectroscopy (XPS), both of which have a time scale of ca. 10^{-16} s, were measured at room temperature and at 80 K. The detailed electronic states of the iron atoms

in the mixed-valence binuclear ferrocene salts are discussed by comparing the results with those obtained in Mössbauer spectroscopy of the same compounds which has a time scale of ca. 10^{-7} s.

Experimental

Commercially available ferrocene was purified by sublimation for the measurements. Other compounds were synthesized following the methods described in Refs. 4–7. The confirmed purities were >99% by means of the melting point, elemental analysis, IR, NMR, and Mössbauer spectroscopy.

Fe K-edge XANES spectra were measured at the National Synchrotron Radiation Research Facility (Photon Factory) affiliated to the National Laboratory for High Energy Physics (KEK-PF). Synchrotron radiation emitted from a storage ring, working at 2.5 GeV and ≈ 160 mA, was monochromated by a Si(311) channel-cut single crystal. The powdery samples were placed between two thin sheets transparent to the X-rays.⁸⁾

XPS spectra were obtained by using Mg K α radiation with a Shimadzu ESCA 750 spectrometer. Binding energy data were calibrated by using the binding energy of Cls photoelectron as the standard (285.5 eV). The experimental error for the binding energy was estimated within ± 0.1 eV.

Results and Discussion

XANES Spectra. Ferrocene and Ferrocenium Triiodide. In the solid state, the molecular symmetry of ferrocene is known to be D_{5d} . Sohn et al. reported that the π orbitals in cyclopentadienyl (Cp) can be classified into the symmetries with the energy levels shown in Fig. 1.⁹⁾ The valence orbitals in iron atoms consist of $e_{2g}(3d)$, $a_{1g}(3d)$, $e_{1g}(3d)$, $a_{1g}(4s)$, $a_{2u}(4p)$, and $e_{1u}(4p)$. The ground state of ferrocene is also known to be $^1A_{1g}(1e_{2g})^4(2a_{1g})^2$. The ground state of the ferrocenium ion is shown to be $^2E_{2g}(1e_{2g})^3(2a_{1g})^2$ by ESR,¹⁰⁾ and by magnetic susceptibility measure-

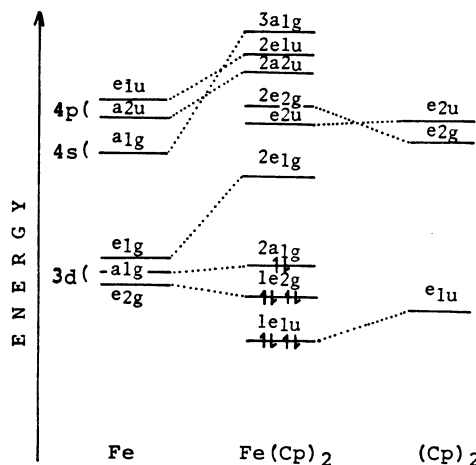


Fig. 1. The estimated relative energy for the molecular orbitals in ferrocene.⁹⁾

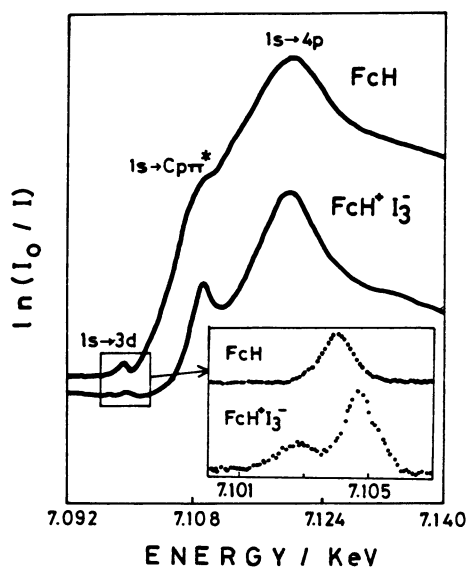


Fig. 2. The XANES spectra of ferrocene and ferrocenium triiodide salt. The $1s \rightarrow 3d$ transitions are given under magnification. The pre-edge continuum background has been subtracted by smoothing the foot of the main peak.

ments.¹¹⁾ This state is slightly split into two Kramers doublets by spin-orbit coupling, indicating a crystal field with a symmetry lower than D_{5d} . However, since the splitting of the two Kramers doublets is estimated to be much smaller than the relevant transition energy, it is neglected in the present investigation.

Figure 2 shows the Fe K-edge XANES spectra of ferrocene and ferrocenium triiodide salt. There is a weak absorption peak below the Fe K-edge ionization threshold, followed by a shoulder on a rising absorption curve which culminates in a strong peak. In the XANES spectrum of ferrocene, the strong peak can be ascribed to the allowed transitions $1s \rightarrow 4p$ e_{1u} or a_{2u} , the lower-energy shoulder to the $1s \rightarrow Cp(\pi^*)$, and

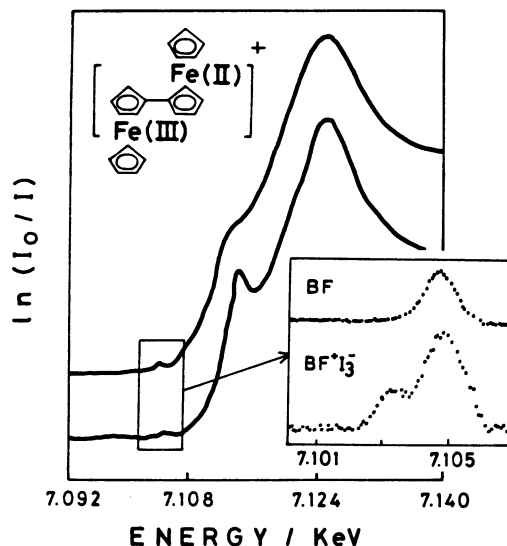


Fig. 3. The XANES spectra of BF and $BF+I_3^-$. The weak $1s \rightarrow 3d$ transition in BF consists of a single peak, while the splitting of 1.57 eV in the $1s \rightarrow 3d$ transition of $BF+I_3^-$ is observed.

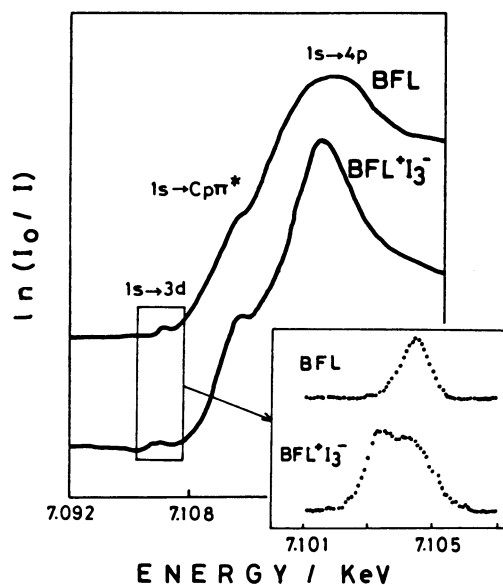


Fig. 4. The XANES spectra of BFL and $BFL+I_3^-$. For $BFL+I_3^-$ the splitting in the $1s \rightarrow 3d$ transition is small and the intensity of the lower energy peak is strong.

the weak pre-edge peak to the dipole-forbidden (quadrupole-allowed or vibronically allowed) transition $1s \rightarrow 3d$ e_{1g} , respectively, based on the relative energy estimated in the molecular orbitals in ferrocene shown in Fig. 1.⁹⁾

The XANES spectrum of ferrocenium ion has been compared with that of ferrocene. In Fig. 2, no energy difference is observed in the intense $1s \rightarrow 4p$ transitions between ferrocene and ferrocenium triiodide salt. On the other hand, there exists a significant difference in the forbidden transition $1s \rightarrow 3d$ between ferrocene and

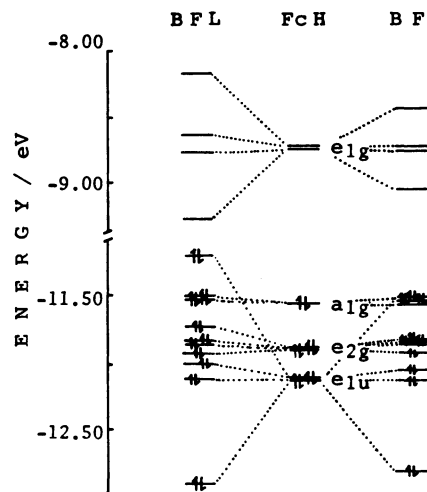


Fig. 5. The total ground-state configuration in the trans (C_{2h}) conformation of BF and in the D_{2h} point group of BFL.¹²⁾

ferrocenium $^+I_3^-$. The weak $1s \rightarrow 3d$ transition in ferrocene consists of a single peak, while a splitting of ca. 2 eV is observed in the $1s \rightarrow 3d$ transition of ferrocenium ion. These results are explained in terms of the crystal field splitting of the ground state. The electronic ground states of the ferrocene and ferrocenium ion are $^1A_{1g}$ and 2E_g consisting of the $a_{1g}^2e_{2g}^4$ and $a_{1g}^2e_{2g}^3$ configurations, respectively. The $1s \rightarrow 3d$ transition of ferrocene is assigned to the transition from the $1s$ orbital to the unoccupied e_{1g} state; in ferrocenium ion, there are two possibilities for the $1s \rightarrow 3d$ transitions from the $1s$ to the unoccupied valence state e_{1g} and e_{2g} . The value of the splitting (ca. 2 eV) in the $1s \rightarrow 3d$ transitions of ferrocenium ion is roughly comparable with the crystal field splitting observed in the electronic absorption data assigned to the d-d transition which corresponds to about 25000 cm^{-1} (ca. 3 eV).¹²⁾

Biferrocene, 1,1'':1',1'''-Biferrocenylene and Their Triiodide Salts. Figures 3 and 4 show the XANES spectra of biferrocene (BF) and 1,1'':1',1'''-biferrocenylene (BFL) compared with their triiodide salts, respectively. The features in the XANES spectra for the neutral species are similar to the spectral feature for ferrocene. Kirchner et al. reported on the molecular orbitals calculated for BF in the trans (C_{2h}) conformation that the net charge on the iron atom and total electron density in each d orbital of BF are similar to those of ferrocene, as shown in Fig. 5.¹²⁾ This result is consistent with the data that the isomer shift and quadrupole splitting in Mössbauer spectra of BF and BFL agree with those of ferrocene.

There is an apparent difference in the $1s \rightarrow 3d$ transition between biferrocenium $^+I_3^-$ ($BF^+I_3^-$) and 1,1'':1',1'''-biferrocenylenium $^+I_3^-$ ($BFL^+I_3^-$), as seen in Figs. 3 and 4 under magnification. The pre-edge continuum background has been subtracted by

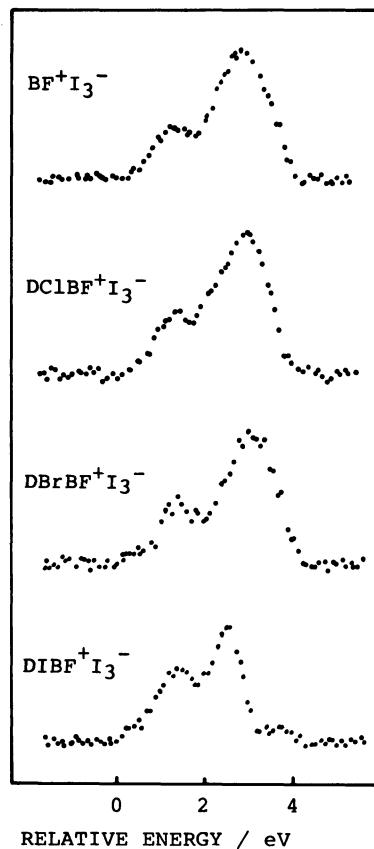


Fig. 6. The $1s \rightarrow 3d$ transition in the XANES spectra for the salts.

smoothing the foot of the main peak. $BF^+I_3^-$, which shows a trapped-valence state in the Mössbauer spectrum, exhibits an asymmetric splitting of 1.57 eV in the $1s \rightarrow 3d$ transition, while $BFL^+I_3^-$, which shows an averaged-valence state in the Mössbauer spectrum, gives a nearly symmetric splitting of 0.89 eV. These transitions are assigned to the transitions from $1s$ to unoccupied molecular orbitals which are mainly ascribed to the $3d$ orbitals corresponding to e_{1g} and e_{2g} in ferrocene.

The splitting in the $3d$ orbital for averaged-valence type, $BFL^+I_3^-$, is found to be smaller than that for trapped-valence type, $BF^+I_3^-$, and the intensity of the lower-energy peak in the $1s \rightarrow 3d$ transition for $BFL^+I_3^-$ is stronger than that for $BF^+I_3^-$. These results are consistent with those obtained in Mössbauer spectroscopy, suggesting that the molecular orbital of $BF^+I_3^-$ differs from that of $BFL^+I_3^-$.

Halogenated Biferrocene Derivatives and Their Triiodide Salts. The features of the XANES spectra for halogenated biferrocenes are also similar to the spectral feature for ferrocene. Figure 6 shows the $1s \rightarrow 3d$ transitions in the XANES spectra for the salts of monooxidized biferrocene ($BF^+I_3^-$), 1',1'''-dichlorobiferrocene ($DCIBF^+I_3^-$), 1',1'''-dibromobiferrocene ($DBrBF^+I_3^-$) and 1',1'''-diiodobiferrocene ($DIBF^+I_3^-$).

The Mössbauer spectrum of $\text{DCIBF}^+\text{I}_3^-$ shows a trapped-valence state, while the Mössbauer spectra of $\text{DBrBF}^+\text{I}_3^-$ and $\text{DIBF}^+\text{I}_3^-$ show averaged-valence states. The XANES spectrum of $\text{DIBF}^+\text{I}_3^-$ is distinguishable from the others by the ratio of the peak intensities and by the separation of the split peaks. Although it is difficult to interpret the XANES spectrum quantitatively for the averaged-valence state, the peculiar XANES spectrum for $\text{DIBF}^+\text{I}_3^-$ can be qualitatively interpreted as a fully delocalized system on two equivalent iron atoms. On the other hand, the XANES spectrum for $\text{DBrBF}^+\text{I}_3^-$ is similar to those of BF^+I_3^- and $\text{DCIBF}^+\text{I}_3^-$, which indicate trapped-valence states in the Mössbauer spectra. The inconsistency of the results obtained from XANES spectra and Mössbauer spectra is explained by assuming that the rate of the thermal electron transfer between the two iron atoms in $\text{DIBF}^+\text{I}_3^-$ is higher than $\text{ca. } 10^{16} \text{ s}^{-1}$ and the rate in $\text{DBrBF}^+\text{I}_3^-$ is higher than $\text{ca. } 10^7 \text{ s}^{-1}$ but lower than $\text{ca. } 10^{16} \text{ s}^{-1}$.

X-Ray Photoelectron Spectroscopy. Since the time scale of XPS is $\text{ca. } 10^{-16} \text{ s}$ comparable with that of XANES, XPS also affords the possibility of distinguishing the localized electronic systems from delocalized ones in the mixed-valence binuclear ferrocenes.¹³⁾ Although the XPS for ferrocene itself and ferrocenium salts has been studied for many years, there are few reports concerning the XPS for the

mixed-valence binuclear ferrocenes. In the present studies, attempts were also made to interpret the XPS spectra of the mixed-valence binuclear ferrocene derivatives in comparison with those of ferrocene and ferrocenium salts.

For ferrocene a sharp band $\text{Fe}2p_{3/2}$ is observed at a binding energy of $\text{ca. } 708 \text{ eV}$, while ferrocenium triiodide has much broader $\text{Fe}2p_{3/2}$ lines at 771 eV due to the exchange interaction of the core electrons with the unpaired valence electrons.¹⁴⁾ In addition, the satellite band with the broad line for ferrocenium ion is observed at 713 eV and is ascribed to the shake-up from the highest occupied orbital to the lowest unoccupied orbital.¹⁴⁾

As shown in Fig. 7, the XPS spectra of the I_3^- salts of monocation of binuclear ferrocenes are found to consist of a single $\text{Fe}2p_{3/2}$ transition peak with a satellite peak. In the XPS spectra for mixed-valence binuclear ferrocenes, it is difficult to distinguish completely a sharp Fe(II) band from an Fe(III) band broadened by the exchange interaction of the core electrons with the valence electrons.

The XPS spectra of BF^+I_3^- , which indicates a trapped-valence state in Mössbauer spectra, are characterized by the main peak in the high energy state and the satellite peak in the low energy state. On the other hand, the satellite band in the spectrum of BFL^+I_3^- which shows an averaged-valence state in Mössbauer spectra becomes broader and of lower energy than that of BF^+I_3^- . The fact that the position of the shake-up satellite band shifts to lower energy indicates that the splitting in the 3d orbitals for averaged-valence compounds is smaller than that for trapped-valence compounds.

Figure 7 shows the XPS spectra for halogenated compounds. In the XPS spectra of $\text{DBrBF}^+\text{I}_3^-$ and $\text{DCIBF}^+\text{I}_3^-$, the satellite bands are clearly observed at the high-energy region as in the case of BF^+I_3^- . On the other hand, the XPS spectrum of $\text{DIBF}^+\text{I}_3^-$ is similar to that of BFL^+I_3^- , although the satellite band is not definitely characterized in the spectrum. These results indicate that two iron atoms of $\text{DIBF}^+\text{I}_3^-$ are equivalent in a delocalized system in the range of the time scale of 10^{-16} s and that the electrons are hopping thermally between the two unequivalent iron atoms in the rate from 10^{-7} s to 10^{-16} s in the case of $\text{DBrBF}^+\text{I}_3^-$.

In the temperature range from 80 K to 298 K , Mössbauer spectra show the trapped-valence states for BF^+I_3^- and $\text{DCIBF}^+\text{I}_3^-$ and the averaged-valence states for BFL^+I_3^- , $\text{DBrBF}^+\text{I}_3^-$ and $\text{DIBF}^+\text{I}_3^-$. The latter are known to give the averaged-valence states even at 4.2 K , whereas BF^+I_3^- becomes an averaged-valence state above 298 K . From the results of Mössbauer, XANES, and XPS data, it can be concluded that the trapped-valence state becomes more stable in the order $\text{DCIBF}^+\text{I}_3^- > \text{BF}^+\text{I}_3^- > \text{DBrBF}^+\text{I}_3^- > \text{DIBF}^+\text{I}_3^-$. This order can neither be explained by the order of electronega-

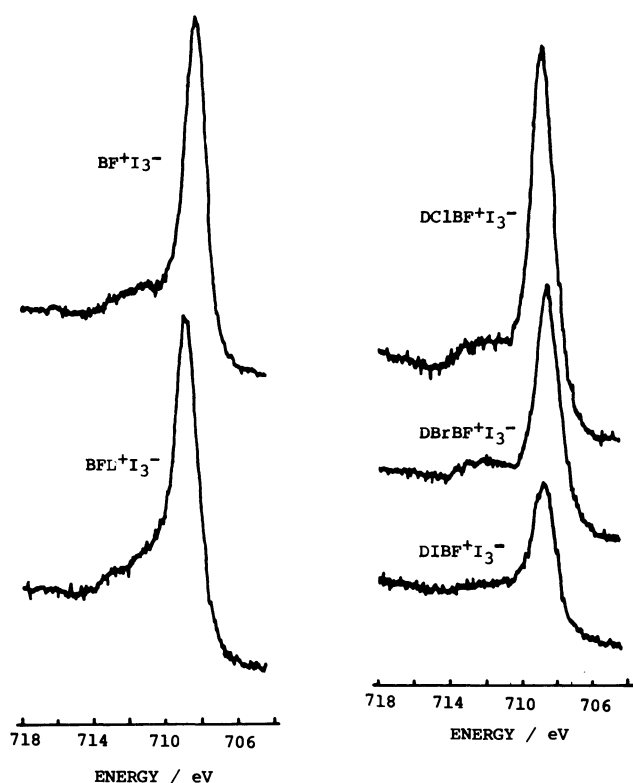


Fig. 7. The $\text{Fe}2p_{3/2}$ XPS spectra of the triiodide salts for binuclear ferrocenes.

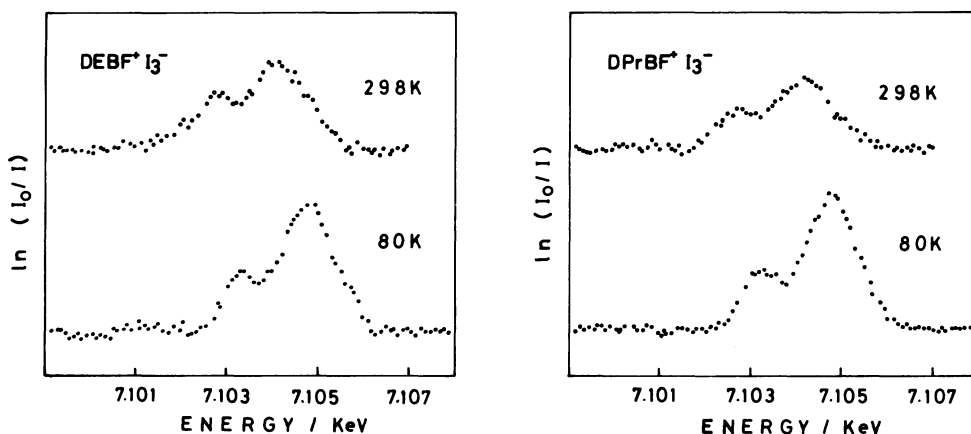


Fig. 8. The temperature dependence of the $1s \rightarrow 3d$ transition in the XANES spectra for $\text{DEBF}^+\text{I}_3^-$ and $\text{DPrBF}^+\text{I}_3^-$.

tivity for the substituted halogen atoms nor by the order of the ionic radii. It can, therefore, be presumed that the difference in electronic state between the two iron atoms is caused by the structural effect of substituents, rather than by their electronic effect.

The most prominent features of the infrared spectra are similar in binuclear ferrocenium ions because of the similarity of the molecular structures. However, there appears to be a difference in the band near 680 cm^{-1} band associated with the fulvalene moiety.¹⁵⁾ The disappearance of the 680 cm^{-1} band in $\text{DIBF}^+\text{I}_3^-$ reveals that the fulvalene moiety has a symmetric structure and the others, whose spectra give strong peaks at ca. 680 cm^{-1} , have an asymmetric fulvalene moiety. Although further structural studies need to be carried out, it would appear that a symmetric molecular structure is indispensable for yielding the averaged-valence state of the iron atoms.

1',1'''-Diethyl- and Dipropylbiferrocene and their Triiodide Salts. It is found that Mössbauer spectra in 1',1'''-diethylbiferrocenium $^+\text{I}_3^-$ ($\text{DEBF}^+\text{I}_3^-$) and 1',1'''-dipropylbiferrocenium $^+\text{I}_3^-$ ($\text{DPrBF}^+\text{I}_3^-$) are temperature dependent, since a trapped-valence state of the iron atoms is observed at low temperatures and an averaged-valence state at room temperature.⁷⁾ The mechanism of this temperature dependence of the Mössbauer spectra has been interpreted by a change of the molecular orbitals accompanying a change in the crystal structure. This is because no-broadening cannot be ascribed to a relaxation effect adopted to the temperature dependence of the Mössbauer spectrum found in *trans*- μ -(as-indacene)bis(cyclopentadienyl-iron).^{7,16)} This interpretation was later supported by the X-ray crystal-structure determination of 1',1'''-dipropylbiferrocenium triiodide at different temperatures.¹⁵⁾ The structural data indicate that the molecular orbitals are influenced more directly by the interaction between the triiodide ion and the ferrocene moiety rather by the intramolecular structural change, especially in the case of the mixed-valence com-

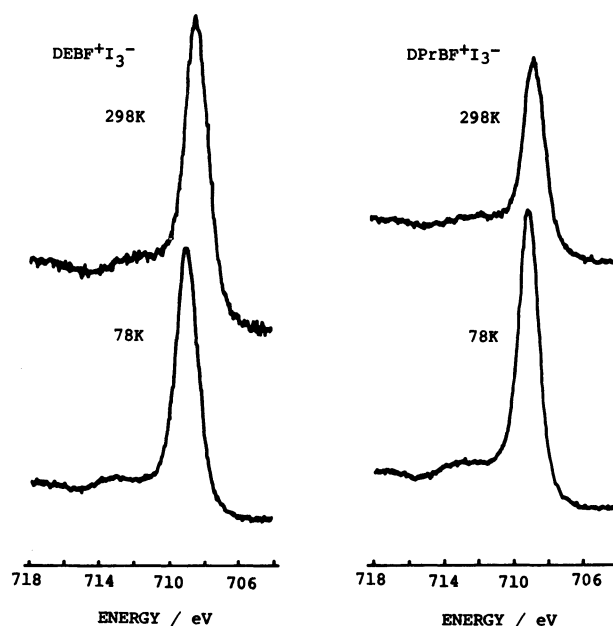


Fig. 9. The temperature dependence of the $\text{Fe}2p_{3/2}$ XPS spectra for $\text{DEBF}^+\text{I}_3^-$ and $\text{DPrBF}^+\text{I}_3^-$.

pounds.

The temperature dependence of the XANES spectra for $\text{DEBF}^+\text{I}_3^-$ and $\text{DPrBF}^+\text{I}_3^-$ is shown in Fig. 8. The XANES spectra at 80 K resemble those of the trapped-valence type compounds, while the spectra at room temperature are similar to those of the averaged-valence type compounds. As shown in Fig. 9, there seems to be a slight temperature dependence of the peak assigned to $\text{Fe}2p_{3/2}$ in XPS spectra for $\text{DEBF}^+\text{I}_3^-$ and $\text{DPrBF}^+\text{I}_3^-$, that is, the satellite peaks are likely to appear at lower temperatures. This dependence is not inconsistent with the results obtained in XANES. These results lead to the conclusion that the temperature dependence of the electronic states for $\text{DEBF}^+\text{I}_3^-$ and $\text{DPrBF}^+\text{I}_3^-$ is explained by assuming a substantial change in the molecular orbital caused by the change of the crystal structure.¹⁵⁾

It is concluded that there are two types of electronic states in the mixed-valence compounds. One is satisfactorily explained by a thermal electron transfer between the two iron atoms in $\text{DBrBF}^+\text{I}_3^-$, because the Mössbauer spectra show the averaged-valence state at the studied temperature, while the feature of XANES and XPS spectra are similar to those for the trapped-valence compounds. The other is interpreted in terms of the substantial change of the molecular orbital caused by the change of the crystal structure at higher temperatures.

The XPS spectra of $\text{I}3\text{d}_{5/2}$ for mixed-valence binuclear ferrocenes are shown in Fig. 10. The XPS spectrum of BF^+I_3^- consists of a single $\text{I}3\text{d}_{5/2}$ transition peak with a shoulder whose intensity is one half that of the main peak. The main peak is assigned to two negatively charged iodine atoms in the terminal position of I_3^- and the shoulder is assigned to an iodine atom at the central position of I_3^- . The charge on the triiodide ion is highly localized and the negatively charged iodine atoms in the terminal position seem to have a significant effect on the electronic states of the ferrocene moiety.

This speculation is supported by the study of the crystal structure for an analogous trapped-valence compound determined by single-crystal X-ray diffraction.^{2,3)} The crystal structure for 1',1'''-dibutylbiferrocenium triiodide at 150 K, whose Mössbauer spectrum shows a trapped-valence state, reveals that one of the negatively charged iodine atoms in the terminal position in a triiodide ion is situated near the ferrocenium-like moiety. It can be presumed that the localization of the molecular orbitals should be caused by such an asymmetric structure between the triiodide ion and the ferrocene moiety.

On the other hand, the XPS spectrum of $\text{I}3\text{d}_{5/2}$ for BFL^+I_3^- , whose Mössbauer spectrum shows the

averaged-valence state, gives an apparently symmetric peak. Since this peak broadens, it can be interpreted as a splitting between the main peak and the side peak in the XPS spectrum of BFL^+I_3^- which is smaller than that of BF^+I_3^- . It can be presumed that the shift of the negative charge on I_3^- in BFL^+I_3^- is insignificant and then the electronic effect of the counter anion on the ferrocene moiety is symmetric, which seems to be favorable to the averaged-valence state.

The XPS spectra of $\text{I}3\text{d}_{5/2}$ for halogenated derivatives are also given in Fig. 10. The spectra for $\text{DCIBF}^+\text{I}_3^-$ and $\text{DBrBF}^+\text{I}_3^-$ are characterized by the broad bands, indicating that there exist various kinds of iodine atoms with different electronic states in the crystal. Unfortunately, the spectra of $\text{DIBF}^+\text{I}_3^-$ cannot be readily interpreted because of the overlap of the spectral components of the iodine atoms of I_3^- and those attached to the Cp rings.

Figure 11 shows the XPS spectra of $\text{I}3\text{d}_{5/2}$ for $\text{DEBF}^+\text{I}_3^-$ and $\text{DPrBF}^+\text{I}_3^-$. These spectra also show broad single peaks both at 78 K and 298 K. It can, therefore, be presumed that a slight difference of the interaction between the triiodide ion and the ferrocene moiety at an increased temperature gives rise to a valence fluctuation in $\text{DEBF}^+\text{I}_3^-$ and $\text{DPrBF}^+\text{I}_3^-$.

The authors are indebted to Dr. Sei'ichiro Iijima, at Research Institute for Polymers and Textiles, for his kind preparation of diethyl- and dipropylbiferrocenium triiodides, and to Professor Takaharu Ohnishi and Dr. Kazunari Domen at Research Laboratory of Resources Utilization, Tokyo Institute of Technology, for their kind help with the use of the X-ray photoelectron spectrometer and the discussion of the results. The authors are grateful to Dr. Masaharu Nomura at National Laboratory for High Energy Physics, and Messrs. Toshihiko Yokoyama, Kiyotaka

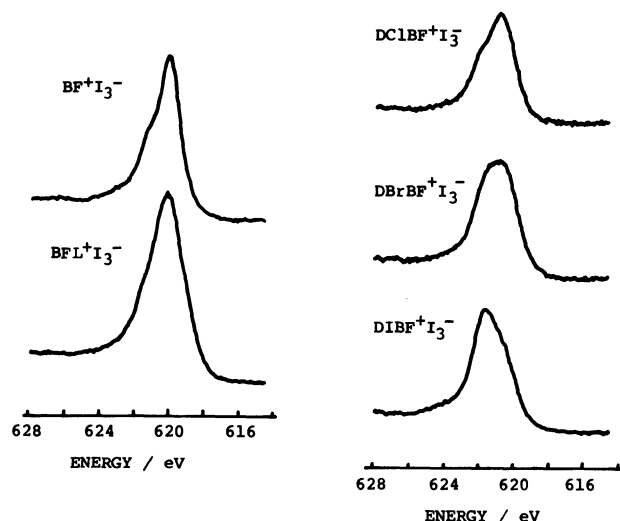


Fig. 10. The XPS spectra of $\text{I}3\text{d}_{5/2}$ for mixed-valence binuclear ferrocenes.

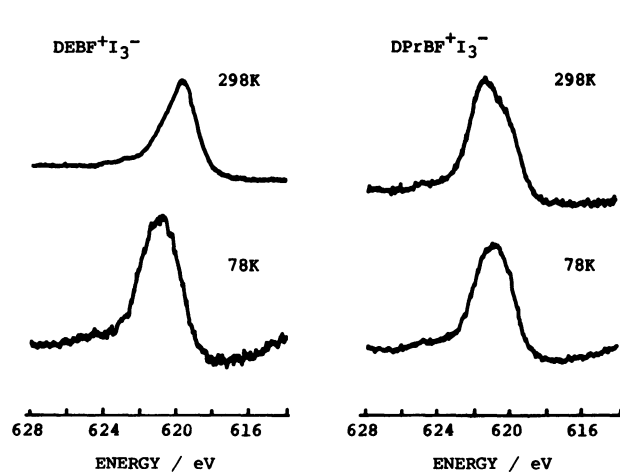


Fig. 11. The temperature dependence of the XPS spectra $\text{I}3\text{d}_{5/2}$ for $\text{DEBF}^+\text{I}_3^-$ and $\text{DPrBF}^+\text{I}_3^-$.

Asakura, and Hiromu Ishii at The University of Tokyo for their help in the experiments at KEK-PF.

References

- 1) I. F. Schegolev, *Phys. Status Solid A*, **12**, 9 (1972); R. H. Holm and J. A. Ibers, "Iron-Sulfur Proteins," ed by W. Lovenberg, Academic Press, New York (1977) Vol. 3, Chap. 7; J. Cambray, R. W. Lane, A. G. Wedd, R. W. Johnson, and R. H. Follm, *Inorg. Chem.*, **16**, 2565 (1977).
- 2) K. Sato, S. Nakashima, M. Watanabe, I. Motoyama, and H. Sano, *Nippon Kagaku Kaishi*, **1985**, 580.
- 3) T.-Y. Dong, D. N. Hendrickson, K. Iwai, M. J. Cohn, S. J. Geib, A. L. Rheingold, H. Sano, I. Motoyama, and S. Nakashima, *J. Am. Chem. Soc.*, **107**, 7996 (1985).
- 4) I. Motoyama, K. Suto, M. Katada, and H. Sano, *Chem. Lett.*, **1983**, 1215.
- 5) F. Kaufman and D. O. Cowan, *J. Am. Chem. Soc.*, **92**, 6198 (1976); D. O. Cowan, R. L. Collins, and F. Kaufman, *J. Phys. Chem.*, **75**, 2025 (1971); D. O. Cowan, G. A. Candela, and F. Kaufman, *J. Am. Chem. Soc.*, **93**, 3889 (1971); D. O. Cowan and J. Park, *Chem. Commun.*, **1971**, 1444.
- 6) W. H. Morrison, Jr. and D. N. Hendrickson, *Inorg. Chem.*, **14**, 2331 (1975); C. LeVanda, K. Bechgaard, D. O. Cowan, U. T. Mueller-Westerhoff, P. Eilbrach, G. A. Candela, and R. L. Collins, *J. Am. Chem. Soc.*, **98**, 3181 (1976).
- 7) S. Iijima, R. Saida, I. Motoyama, and H. Sano, *Bull. Chem. Soc. Jpn.*, **54**, 1375 (1981).
- 8) H. Oyanagi, T. Matsushita, M. Ito, and H. Kuroda, KEK Report, KEK83 (1984).
- 9) Y. S. Sohn, D. N. Hendrickson, and H. B. Gray, *J. Am. Chem. Soc.*, **92**, 3233 (1970).
- 10) R. Prins and F. J. Reinders, *J. Am. Chem. Soc.*, **91**, 4929 (1969); A. H. Maki and T. E. Berry, *ibid.*, **87**, 4437 (1965).
- 11) D. O. Cowan, C. LeVanda, R. L. Collins, G. A. Candela, U. T. Mueller-Westerhoff, and P. Eilbrach, *J. Chem. Soc., Chem. Commun.*, **1973**, 329.
- 12) P. F. Kirchner, G. H. Loew, and U. T. Mueller-Westerhoff, *Inorg. Chem.*, **15**, 2665 (1976).
- 13) C. LeVanda, K. Bechgaard, D. O. Cowan, U. T. Mueller-Westerhoff, P. Eilbrach, G. A. Candela, and R. L. Collins, *J. Am. Chem. Soc.*, **98**, 3181 (1976).
- 14) P. C. Healy and A. H. White, *Chem. Commun.*, **1971**, 1444.
- 15) M. Konno, S. Hyodo, and S. Iijima, *Bull. Chem. Soc. Jpn.*, **55**, 2327 (1982).
- 16) S. Iijima, I. Motoyama, and H. Sano, *Bull. Chem. Soc. Jpn.*, **53**, 3130 (1980).